11th Hungarian Conference on Theoretical and Applied Mechanics
HCTAM, 2011
August 29-31, 2011 Miskolc, Hungary

FLOW AROUND AN OSCILLATING OR ORBITING CYLINDER – COMPARATIVE NUMERICAL INVESTIGATION

Betti Bolló[1] and László Baranyi[2]

[1]Department of Fluid and Heat Engineering, University of Miskolc
3515 Miskolc-Egyetemváros, Hungary
aramzb@uni-miskolc.hu

[2]Department of Fluid and Heat Engineering, University of Miskolc
3515 Miskolc-Egyetemváros, Hungary
arambl@uni-miskolc.hu

Abstract: *The two-dimensional flow around a circular cylinder oscillated in in-line or transverse directions or following an orbital path at a Reynolds number of 140 is investigated numerically using two different methods: a 2D in-house code based on a finite difference solution (FDM) and the commercial software FLUENT, based on the finite volume method (FVM). Computations are carried out at a frequency ratio of $f/St_0=0.9$ for different oscillation amplitude values in the lock-in domain. Both methods analyze flow properties such as drag, lift and mechanical energy transfer between the fluid and the cylinder for both transverse, in-line or orbital cylinder motions. Computational results obtained using the two methods agree well for both type of cylinder motions.*
Keywords: *circular cylinder, in-line oscillation, mechanical energy transfer, orbital motion, oscillatory flow, transverse oscillation*

1. INTRODUCTION

The flow around a stationary cylinder placed in a uniform stream is a classical bluff body problem in fluid mechanics. Its physical and real-life applications (for example: chimney stacks, offshore structures and risers, cables of suspended bridges, transmission lines, etc.) have attracted the attention of engineers and scientists for over a century, leading to many theoretical, experimental and numerical investigations, summarized in [1].

Topics relevant to the current study are forced in-line, transverse and orbital cylinder oscillation in a uniform stream, and oscillatory flow. The phenomena still have some unanswered questions with physical relevance. The flow around a transverse oscillating circular cylinder has been studied extensively with a focus on the shedding regime, phase angle between body displacement and transverse force [2-4].

Extensive studies have been performed for in-line forced cylinder motion; examples are [5], in which two-dimensional (2D) numerical simulations are conducted at a Reynolds number of 200 over a wide frequency ratio using an accurate spectral finite-difference method; and [6], where a mathematical model is developed for the investigation of dynamical bifurcation behavior.

In practice, it can happen that the circular cylinder oscillates in transverse and in-line directions simultaneously. Experimental evidence (see e.g., [7]) shows that where the ratio of the mass of the oscillating system and that of the displaced fluid (i.e., mass ratio) is high (e.g. vibrating structures in air), then the frequencies of in-line oscillation and transverse oscillation are approximately equal to each other. In this case the cylinder is following an elliptical path. Such orbital motion has been investigated for example by [8, 9].

This numerical study investigates the effect of oscillation amplitude on the flow around a circular cylinder oscillating transversely, in-line or orbitally at a given Reynolds number and frequency ratio. The main purpose of the present study is to compare results from two very different CFD methods in order to further support previous findings [9-12]. The first author used the commercial software FLUENT, based on the finite volume method (FVM). The second author used his own finite difference method (FDM) code using boundary-fitted coordinates. Both methods analyze flow properties such as drag, lift and torque coefficients, and mechanical energy transfer between the fluid and the cylinder.

2. COMPUTATIONAL METHODS

For the 2D in-house FDM code a non-inertial system fixed to the cylinder is used for the computation of the 2D low-Reynolds number unsteady flow around a circular cylinder placed in a uniform stream and forced to oscillate in in-line and/or transverse directions. The governing equations are the non-dimensional Navier-Stokes equations for incompressible constant-property Newtonian fluid, the equation of continuity and the Poisson equation for pressure. The convective terms are calculated using a third-order modified upwind scheme [9]. On the cylinder surface, no-slip boundary condition is used for the velocity and a Neumann type boundary condition is used for the pressure. Potential flow is assumed in the far field, and also potential flow is used as an initial condition except for the cylinder surface, where zero velocity is used [9].

For FVM simulations Ansys Fluent v13.0 commercial software was used for the solution of the two-dimensional low-Reynolds number, unsteady, incompressible, constant-property oscillatory fluid flow for the collocated grid arrangement. The second order upwind scheme was used to discretize the convective terms in the momentum equations. The semi-implicit method for the pressure linked equations (SIMPLE) scheme is applied for solving the pressure-velocity coupling. On the cylinder surface no-slip boundary condition is prescribed. In the far field uniform velocity distribution is used as an initial condition except for the cylinder surface, where the velocity is zero.

For both FDM and FVM computations the computational domain is characterized by two concentric circles: the inner represents the cylinder surface with radius R_1, the outer the far field with radius R_2. The origin of the coordinate system is in the centre of the cylinder. The positive x axis is directed downstream. The computational domain size is R_2/R_1=60 with corresponding mesh points of 361x236 (azimuthal x radial), respectively. In the physical domain logarithmically spaced radial cells are used, providing a fine grid scale near the cylinder wall and a coarse grid in the far field. A dimensionless time step of Δt=0.0005 is used for the FDM, and Δt=0.001 for the FVM. Both methods have been extensively tested against experimental and computational results [9, 13] and very good agreement was found for both methods.

The accuracy of numerical results is compared by means of integral quantities such as lift C_L and drag C_D coefficients. The drag and lift coefficients are calculated as

$$C_L = \frac{2F_L}{\rho U^2 D}, C_D = \frac{2F_D}{\rho U^2 D}, \tag{1}$$

where ρ is the fluid density, U is the free-stream velocity, D is the cylinder diameter, F_L and F_D is the lift and drag force per unit length of the cylinder. The time-mean (TM) and root-mean-square (rms) values of the lift and drag coefficients are defined as

$$\overline{C} = \frac{1}{nT}\int_{t_1}^{t_1+nT} C(t)dt,\ C_{rms} = \sqrt{\frac{1}{nT}\int_{t_1}^{t_1+nT}\left[C(t)-\overline{C}\right]^2 dt}, \tag{2}$$

where T is a period of a vortex shedding, n is the number of periods. The general coefficient C stands for drag and lift coefficients. Unless otherwise indicated the lift and drag coefficients shown in this study do not contain inertial forces originating from the system fixed to the accelerating cylinder. Coefficients obtained by removing the inertial forces are often termed 'fixed body' coefficients [3]. The relationship between the two sets of coefficients can be written as

$$C_L = C_{Lfb} + \frac{\pi}{2} a_{0y},\quad C_D = C_{Dfb} + \frac{\pi}{2} a_{0x}, \tag{3}$$

where subscript *fb* refers to the fixed body [14]. Here a_{0x} and a_{0y} are the dimensionless x and y components of cylinder acceleration. Since these accelerations are periodic their time-mean values vanish, resulting in identical TM values for the two setups. Equation (3) shows that for in-line motion the two lift coefficients are identical, while the drag coefficients are different from each other. For transverse cylinder motion it is exactly the other way round.

The torque coefficient t_q (positive in counter-clockwise direction) is non-dimensional torque originating from the shear stress acting on the cylinder surface:

$$t_q = \frac{1}{4Re}\int_0^{2\pi} \omega_0(\psi)d\psi, \tag{4}$$

where ψ is the polar angle and ω_0 is the dimensionless vorticity [12].

3. RESULTS

The FDM code is set up for a mechanically oscillated cylinder placed in a uniform stream, while the FVM simulation is for oscillatory flow around a stationary cylinder. However, when viewed from a system fixed to the cylinder, these two cases are kinematically identical (though dynamically not) and can thus be compared. The non-dimensional cylinder displacement of the centre of the cylinder is described by

$$x_0(t) = A_x \cos(2\pi f_x t),\quad y_0(t) = -A_y \sin(2\pi f_y t), \tag{5}$$

where t is the non-dimensional time, and f_x, f_y and A_x, A_y are the non-dimensional amplitudes and frequencies of cylinder oscillation in in-line and transverse directions, respectively. The non-dimensional frequency f_y=0 for in-line oscillations, f_x=0 for transverse oscillations and the two frequencies are identical for orbital cylinder motion, that is, f= f_x= f_y. Here the oscillation frequency was set at f=0.9St$_0$=0.16389 for all three type of motions, where St$_0$ is the non-dimensional vortex shedding frequency, or Strouhal number, for a stationary cylinder at Re=140. This frequency ratio value ensures that lock-in condition can be reached at a moderate amplitude values. Lock-in or synchronization happens when the vortex shedding frequency synchronizes with the frequency of cylinder motion. In this study only locked-in cases were considered. Equation (5) yields a clockwise orbit. A

counterclockwise orbit can be obtained if the negative sign in y_0 is changed into positive. In this study clockwise cylinder orbit is assumed.

3.1. In-line oscillation

The non-dimensional cylinder displacement of the centre of the cylinder for an in-line cylinder motion is obtained from Eq. (5) in the limiting case when the transverse amplitude A_y tends to zero. For this case, when TM values of lift and torque coefficients are plotted against A_x, sudden changes in state (jumps) are found at some amplitude values [11].

Figure 1(a) shows the TM of lift (and the identical fixed body lift; see Eq. (3)) against the oscillation amplitude A_x for both methods at Re=140, and the TM of torque is shown in Fig. 1(b). As can be seen in these figures, the solution jumps between two states, and the two state curves are mirror images of each other, as was found earlier in [12]. The state curves compare well but the location and number of jumps are different, [15]. The rms values plotted against amplitude yield no jumps, as also shown in [11]. FDM and FVM rms results obtained for these cases (not shown here) also compare well.

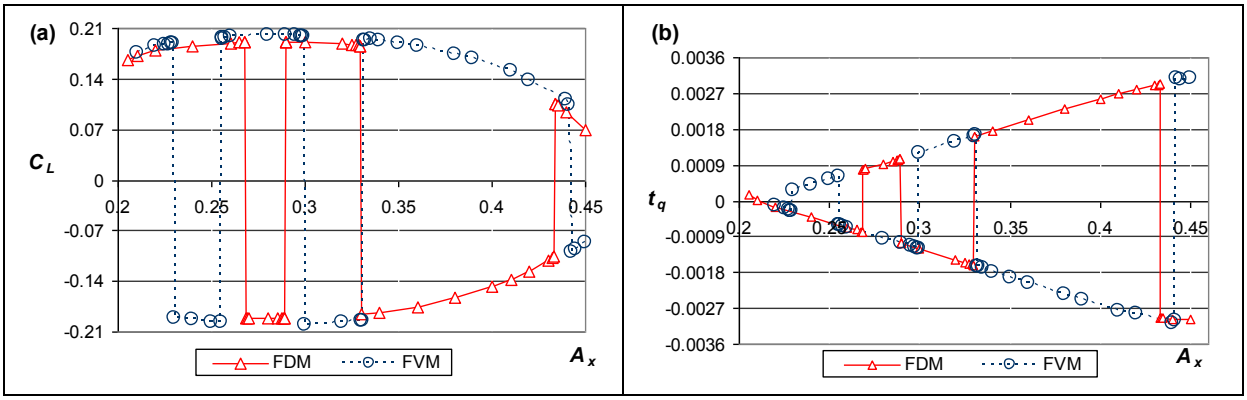

Figure 1. Time-mean of lift (a) and torque (b) versus amplitude A_x

3.2. Transverse oscillation

The transverse cylinder motion can be considered as the limiting case of an orbiting cylinder, when the amplitude of in-line oscillation A_x tends to zero. TM and rms values of force coefficients (C_L, C_D, t_q) when plotted against amplitude A_y does not result in any jumps as shown in [11].

Only two sets of curves will be shown for transverse cylinder oscillation. Figure 2 shows the TM and rms values of the drag (and fixed-body drag at the same time) coefficient obtained by FDM and FVM. It can be seen that the agreement between the results of the two methods is very good; see also [15].

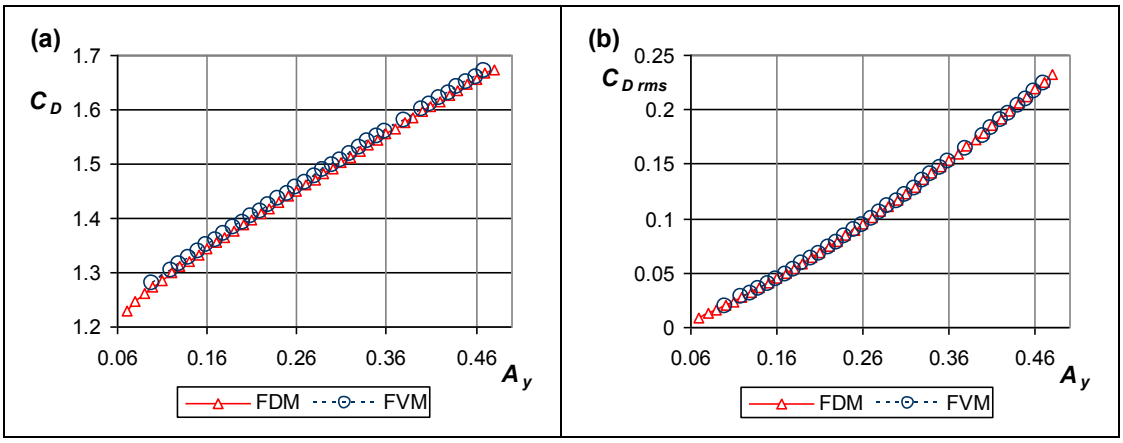

Figure 2. Time-mean of drag (a) and rms of fixed body drag (b) versus amplitude A_y

3.3. Orbital motion

The orbital motion of the cylinder is created by the superposition of two forced oscillations with identical frequencies of $f_x = f_y$. The frequency of f=0.9St$_0$ is used here. The motion of the centre of the cylinder is defined by Eq. (5), where non-zero A_x and A_y amplitudes give an elliptical motion. During each set of computations, the in-line amplitude A_x is fixed at a value of 0.4, and the transverse amplitude A_y values are varied. When TM and rms values of force coefficients (lift, drag or torque) are plotted against oscillation amplitude, two state curves

are found for all force coefficients and the real solutions jump between these state curves. The location and number of jumps are identical for all curves [9].

Figure 3(a) shows the TM of lift (and the identical fixed body lift) against the oscillation amplitude at f=0.9St$_0$ and Re=140. It was found that for in-line motion the location and number of jumps obtained using the two methods are usually different, but here the number of jumps is identical, while the location of jumps is slightly different. Figure 3(a) corresponds to a typical case of approximately parallel state curves shown in [9] for a cylinder orbiting counterclockwise. The values of C_{Lrms} and C_{Lfbrms} are not identical for orbital motion, but the state curves are similar. The rms of the fixed body lift coefficient is shown in Fig. 3(b), which corresponds to the diverging state curves shown in [9]. In this case the state curves intersect each other at zero A_y value, which corresponds to the limiting case of in-line cylinder motion. The two methods compare well again.

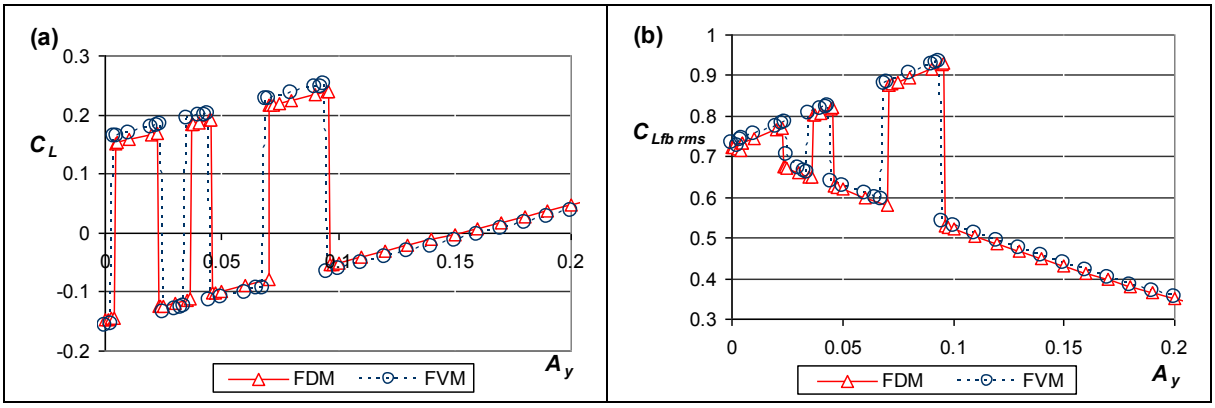

Figure 3. Time-mean of lift (a) and rms of fixed body lift (b) versus amplitude A_y at A_x=0.4

For orbital motion jumps can be found not only in the TM of lift and drag but in all TM and rms curves [9]. The TM of drag coefficient (identical with the TM of fixed body drag) is shown in Fig. 4(a). The FDM and FVM curves seem to differ quite substantially, but the average deviation between the two curves is just 0.96%. Using a larger computational domain would probably reduce the discrepancy between the two curves further. Figure 4(b) shows the rms of fixed body drag coefficient. As can be seen in the figure, the location and number of jumps are practically identical for the two methods. The agreement between the two sets of results is good.

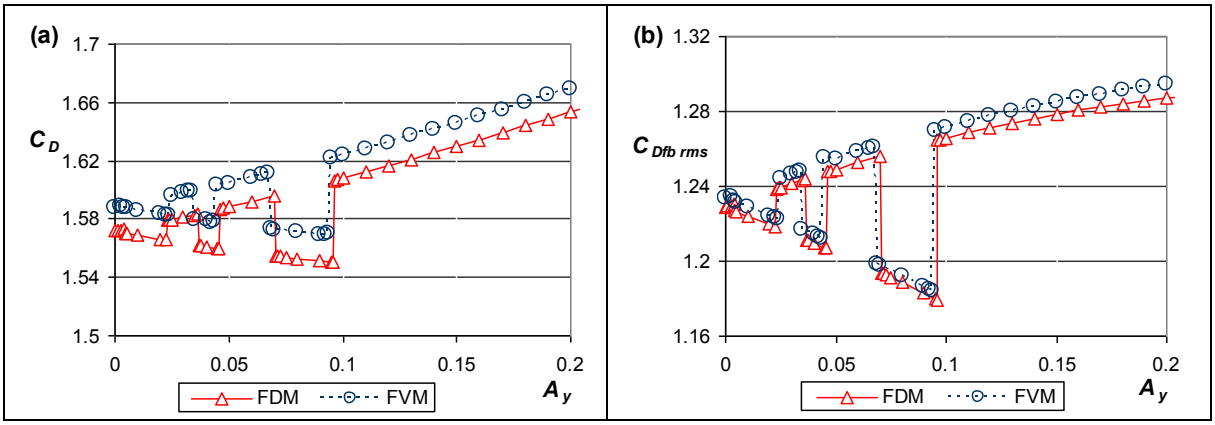

Figure 4. Time-mean of drag (a) and rms of fixed body drag coefficient (b) versus amplitude A_y at A_x=0.4

Let us investigate now the vicinity of a jump using FVM. Limit cycle curves (y_0,C_L) are shown in Fig. 5(a) for pre- and post jump amplitude values of A_{y1}=0.0032 and A_{y2}=0.0038. As can be seen, not only the difference between the transverse amplitude values is small but the amplitude values are small themselves, meaning that, although orbital, the cylinder motion is close to the limiting case of in-line oscillation. The figure shows that the pre-jump curve (thin line) is nearly the mirror image of the post-jump curve (thick line) and the directions of orientation of the two curves are opposite. A tiny change in the amplitude causes a drastic change in the limit cycle (y_0,C_L). Figure 5(b) shows the limit cycle curves (x_0,C_D) for the same amplitude values. The pre- and post-jump curves obtained using FDM and FVM coincide and the directions of orientation of the two curves are identical. As can be seen in Figs. 5(a) and (b), in contrast with the dramatic effect of the small change in the amplitude on the limit cycle curve (y_0,C_L), the same amplitude change hardly influences limit cycle curve (x_0,C_D).

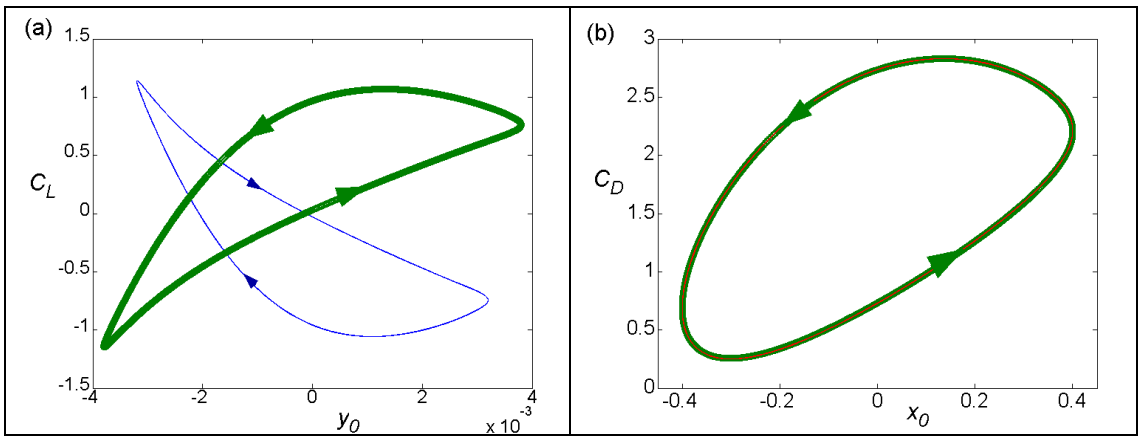

Figure 5. Limit cycle curves (y_0,C_L) (a) and (x_0,C_D) (b); thin line: A_{y1}=0.0032; thick line: A_{y2}=0.0038

The limit cycle curves (C_D,C_L) are shown in Fig. 6 for the same amplitude values as before. In the figure the pre-jump curve (thin line) is the mirror image of the post-jump curve (thick line) and even the directions of orientation of the two curves are opposite. Again, a small amplitude change resulted in large change in the limit cycle curve.

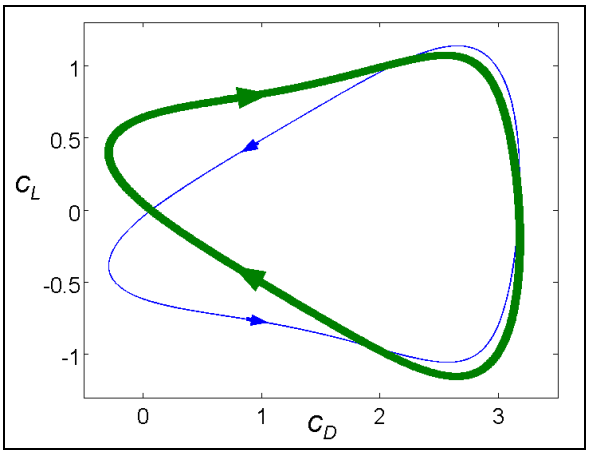

Figure 6. Limit cycle curves (C_L,C_D); thin line: A_{y1}=0.0032; thick line: A_{y2}=0.0038

Figure 7(a) shows the transient part of the time-history of lift for the same pre- and post-jump amplitude values as earlier, using FVM data. It can be seen in the figure that the two solutions are identical while the wake flow is steady, but then they begin to diverge and become more periodic by around the dimensionless time of t=60. The fully periodic state is shown in Fig. 7(b), where the curves appear to be mirror images of each other.

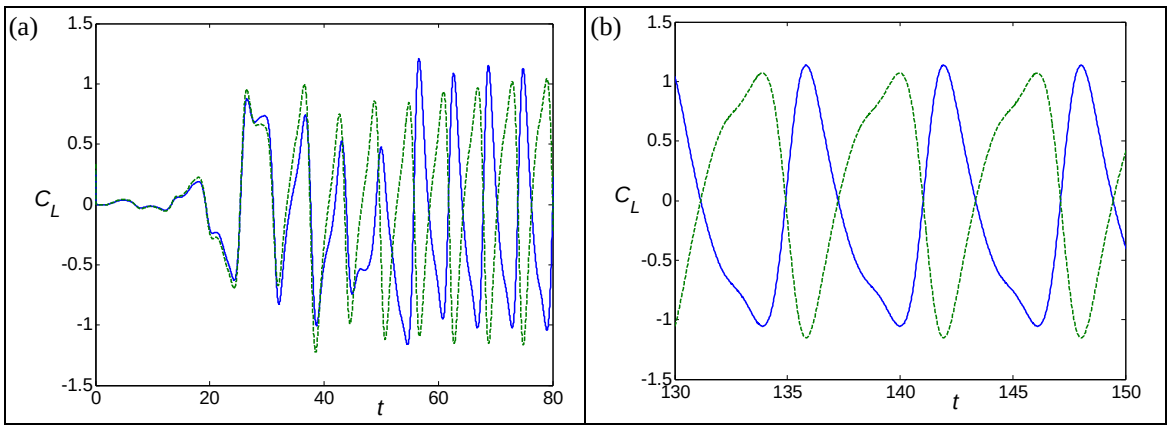

Figure 7. The time-history of lift; transition (a), periodic (b); solid line: A_{y1}=0.0032, dotted line: A_{y2}=0.0038

3.4. Mechanical energy transfer

Both methods were used to analyze the mechanical energy transfer between the fluid and the cylinder. The mechanical energy transfer for transverse cylinder motion was defined in [4] and it was extended for two-degree-of-freedom cylinder motion in [9]. The mechanical energy transfer E can be divided into two parts,

$$E = E_1 + E_2\,, \tag{6}$$

where E_1 and E_2 are the mechanical energy transfer for transverse and in-line motion, respectively, and can be written as follows:

$$E_1 = \int_0^T C_L(t)\dot{y}_0(t)dt\,,\ E_2 = \int_0^T C_D(t)\dot{x}_0(t)dt\,, \tag{7}$$

where T is the motion period, x_0 and y_0 represent the dimensionless displacement of the cylinder in x and y directions, respectively. The over dot denotes differentiation by dimensionless time.

Figure 8(a) shows the mechanical energy transfer E for in-line oscillation (E=E_2, see Eq. (7)) against oscillation amplitude A_x. The mechanical energy transfer is found to be negative for the lock-in domain investigated, and the magnitude of E increases with increasing amplitude. In [9] it was also found that the energy transfer E_2 – originating from the in-line cylinder motion – was negative in the investigated amplitude domain. This means that the fluid acts against the cylinder motion, with a dampening effect.

The energy transfer (E=E_1) for transverse cylinder motion is shown in Fig. 8(b). The value of E first increases and then steeply decreases with increasing amplitude values. The value of energy transfer E can be either positive or negative as a function of oscillation amplitude. The energy transfer curve has a local maximum at around A_y=0.31. Positive E values mean that energy is added to the cylinder from the fluid, and so flow-induced vibration is liable to occur if the cylinder is elastically supported. The two CFD methods yield practically the same energy transfer results for both in-line and transverse cases.

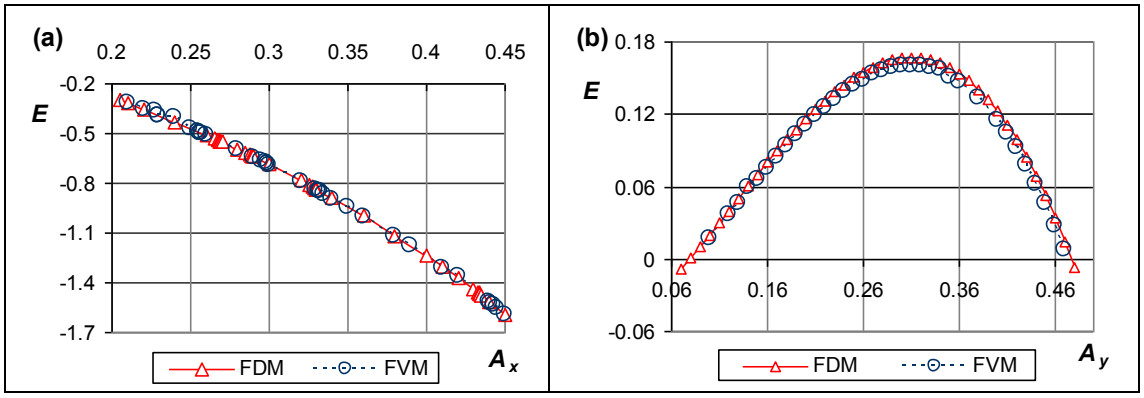

Figure 8. Mechanical energy transfer versus amplitude A_y; in-line (a) transverse (b) oscillation

Figures 9 and 10 show the mechanical energy transfer between the fluid and the cylinder against transverse amplitude A_y for orbital cylinder motion using both CFD methods. Figure 9 shows the energy transfer for transverse E_1 (a) and for in-line motion E_2 (b). For both energy transfer coefficients jumps are found, as also shown in [9], and the number and location of jumps are identical with those of in the TM and rms values of force coefficients belonging to the same parameters (Re, f, A_x, A_y) shown Fig. 3 (see also [9]). The value of energy transfer E_1 jumps between positive and negative values. Naturally, here the value of E_2 is also negative, as it is for the in-line cylinder motion (see Fig. 8(a)).

Figure 10 shows the total mechanical energy transfer E for orbital motion, which is the sum of E_1 and E_2 shown in Fig. 9. The agreement between the two sets of results obtained by FDM and FVM is very good.

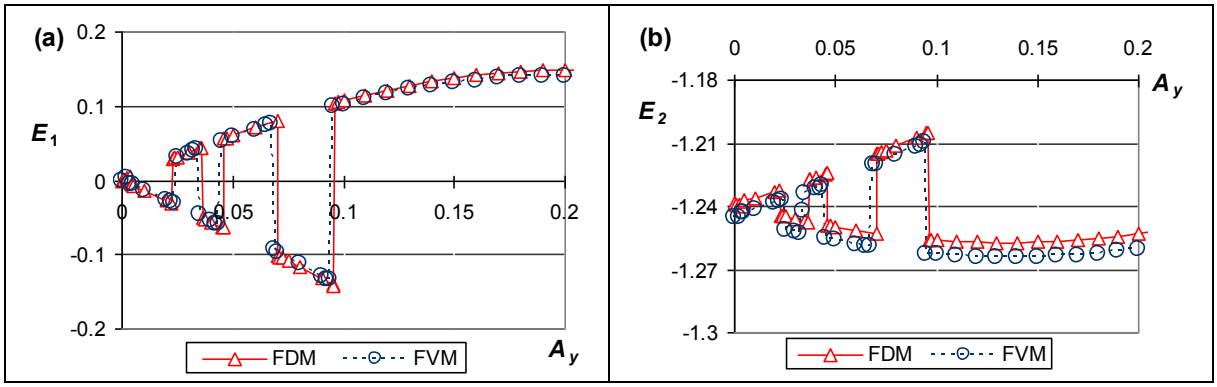

Figure 9. Mechanical energy transfer versus amplitude A_y for orbital motion; E_1 (a), E_2 (b) at Re=140

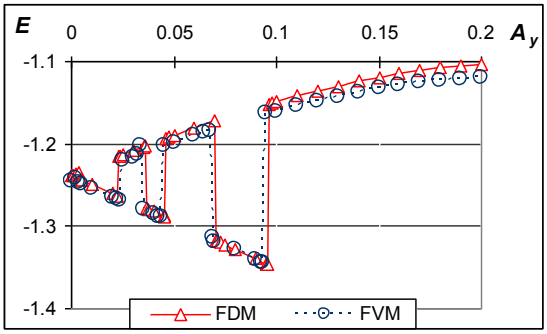

Figure 10. Mechanical energy transfer versus amplitude A_y for orbital motion

4. CONCLUSIONS

Two CFD methods (FVM and FDM) were used to simulate 2D low Reynolds number flow (Re=140) past an oscillating cylinder at frequency ratio f=0.9St$_0$ and an equivalent oscillatory flow past a stationary cylinder. Computational results obtained using both methods agree well for in-line, transverse and orbital cylinder motions.

State curves, in-line motion: FDM and FVM yield the same state curves. Jumps between them appear in different locations and numbers. For orbital motion the number of jumps is identical and the locations also correspond closely.

Energy transfer: for in-line motion results are always negative (flow acts against cylinder motion), while for transverse oscillation both positive (enhancing cylinder motion) and negative values occur. For orbital motion values of energy transfer are negative and jumps appear in the state curves.

The good agreement gained for all aspects investigated serves to act as supporting evidence for earlier findings from FDM studies [9, 12]. Further studies will include the investigation of flow at further Reynolds numbers and frequency ratios for larger domain size.

ACKNOWLEDGEMENTS

The support provided by the Hungarian Research Foundation (OTKA Projects K 76085 and K 68207) is gratefully acknowledged. The work was carried out as part of the TÁMOP-4.2.1.B-10/2/KONV-2010-0001 project in the framework of the New Hungarian Development Plan. The realization of this project is supported by the European Union, co-financed by the European Social Fund.

REFERENCES

1. M. M. Zdravkovich. *Flow around circular cylinders. Vol.1: Fundamentals.* Oxford University Press, Oxford, 1997.
2. C. H. K. Williamson and A. Roshko. Vortex formation in the wake of an oscillating cylinder. *Journal of Fluids and Structures*, 2:355-381, 1988.
3. X.Y. Lu and C. Dalton. Calculation of the timing of vortex formation from an oscillating cylinder. *Journal of Fluids and Structures*, 10:527-541, 1996.
4. H. M. Blackburn and R. D. Henderson. A study of two-dimensional flow past an oscillating cylinder. *Journal of Fluid Mechanics*, 385:255-286, 1999.
5. Q. M. Al-Mdallal, K. P. Lawrence and S. Kocabiyik. Forced streamwise oscillations of a circular cylinder: Locked-on modes and resulting fluid forces. *Journal of Fluids and Structures*, 23:681-701, 2007.
6. N. W. Mureithi, K. Huynh, M. Rodriguez and A. Pham. A simple low order model of forced Karman wake. *International Journal of Mechanical Sciences*, 52:1522-1534, 2010.
7. N. Jauvtis and C. H. K. Williamson. The Effect of Two Degrees of Freedom on Vortex-Induced Vibration and at Low Mass and Damping. *Journal of Fluid Mechanics*, 509:23-62, 2004.
8. E. Didier and A. R. J. Borges. Numerical predictions of low Reynolds number flow over an oscillating circular cylinder. *Journal of Computational and Applied Mechanics*, 8(1):39-55, 2007.
9. L. Baranyi. Numerical simulation of flow around an orbiting cylinder at different ellipticity values. *Journal of Fluids and Structures*, 24:883-906, 2008.
10. L. Baranyi. Numerical simulation of flow past a cylinder in orbital motion. *Journal of Computational and Applied Mechanics* 5(2):209-222, 2004.
11. L. Baranyi. Sudden and gradual alteration of amplitude during the computation for flow around a cylinder oscillating in transverse or in-line direction. *ASME 2009 Pressure Vessels and Piping Conference, Symposium on Flow-Induced Vibration*, Prague, Paper No. PVP2009-77463, 2009.
12. L. Baranyi, K. Huynh and N. W. Mureithi. Dynamics of flow behind a cylinder oscillating in-line for low Reynolds numbers. *Proc. 7th International Symposium on Fluid-Structure Interactions, Flow-Sound Interactions, and Flow-Induced Vibration and Noise,* (*ASME Conference*), Montreal, Québec, Canada, Paper No. FEDSM-ICNMM2010-31183, 2010.
13. B. Bolló and L. Baranyi. Computation of low-Reynolds number flow around a stationary circular cylinder. *Proc. 7th International Conference on Mechanical Engineering,* Budapest, pp. 891-896, 2010.
14. L. Baranyi. Lift and drag evaluation in translating and rotating non-inertial systems. *Journal of Fluids and Structures,* 20(1):25-34, 2005.
15. B. Bolló and L. Baranyi. Computation of low-Reynolds number flow around an oscillated circular cylinder. *Proc. 25th MicroCAD, International Scientific Conference*, Miskolc, Hungary, Section D, pp. 19-24, 2011.